AD-A250 672

(2)

OFFICE OF NAVAL RESEARCH

GRANT NO. N00014-91-J-1447
R&T CODE 414044

Technical Report No. 19

# TRIISOPROPYLINDIUM, A NEW PRECURSOR FOR OMVPE GROWTH

by

C. H. CHEN, C. T. CHIU, and G. B. STRINGFELLOW

20030220185



Prepared for Publication

in the

Journal of Crystal Growth

University of Utah
Dept. of Materials Science & Engineering
Salt Lake City, UT 84112

May 22, 1992



92-13836

92 5 26 051

# Triisopropylindium for OMVPE Growth

C.H. Chen, C.T. Chiu, G.B. Stringfellow

Department of Materials Science and Engineering
University of Utah
Salt Lake City, UT 84112

R.W. Gedridge, Jr.

Chemistry Division
Research Department
Naval Air Warfare Center
China Lake, CA 93555

## Abstract

The organometallic vapor phase epitaxial (OMVPE) growth of In-containing III-V semiconductors typically uses trimethylindium (TMIn). However, TMIn suffers from several problems. First, it is well known that the effective vapor pressure of solid TMIn changes with time because of changes in the surface area. Secondly, TMIn decomposes slowly for temperatures lower than 400 °C in an atmospheric pressure OMVPE reactor; it is too stable for some low-temperature applications. In addition, it causes carbon contamination, especially at low temperatures, due to the $CH_3$ radicals. Thus, there is a need for new In precursors that are liquids at room temperature and do not contain $CH_3$ radicals. This work reports the first decomposition and OMVPE growth studies for a newly developed indium source, triisopropylindium (TIPIn). The decomposition was carried out in an isothermal flow tube reactor with the reaction products analyzed using a mass spectrometer. The temperature for 50% decomposition is ~110 °C for TIPIn in a He ambient. This is about 200 °C lower than that for TMIn under similar conditions. The mass spectroscopic peaks occur at m/e=39, 42, 43, 71, and 86, indicating that the major product for TIPIn decomposition is $C_6H_{14}$. This suggests that TIPIn decomposes by homolysis, producing $C_3H_7$ radicals that recombine to produce $C_6H_{14}$. The OMVPE growth study was carried out in an atmospheric pressure OMVPE reactor in $H_2$ with $AsH_3$ as the As source. InAs epilayers with good surface morphologies were obtained for temperatures as low as 300 °C at a V/III ratio of 460. The necessary V/III ratio increases as the growth temperature is decreased, due to the incomplete decomposition of $AsH_3$ at low temperatures. The as-grown epilayers are n-type, with $n=1\times10^{17}$ $cm^{-3}$ for substrate temperatures of 500 and 400 °C. The electron concentration increases as the

growth temperature is lowered below 400 °C. However, n is less than for InAs grown using TMIn and $AsH_3$. The residual donor may be a volatile impurity in the TIPIn. More likely, it is carbon from the isopropyl radicals. The less reactive $C_3H_7$ radicals produce far less carbon than the more reactive $CH_3$ radicals produced by TMIn pyrolysis. The InAs growth efficiency is low as compared to that for InAs grown using TMIn and $AsH_3$ in the diffusion-limited regime. This is mainly caused by TIPIn decomposition upstream from the substrate because of the very low pyrolysis temperatures. Thus, TIPIn may be best suited for low pressure OMVPE or, particularly, for chemical beam epitaxy.

## 1. INTRODUCTION

In the early development of organometallic vapor phase epitaxy (OMVPE), the growth of In-containing alloys was plagued by parasitic reactions between the most common precursor, triethylindium (TEIn), and the group V hydride sources [1]. Later, it was found that parasitic reactions were reduced using low reactor pressures [2]. The problem was finally resolved when trimethylindium (TMIn) was introduced as the indium precursor [3, 4]. Today, high quality indium-containing alloys are routinely produced with high growth efficiencies [5].

However, some problems still exist with the use of TMIn: (1) OMVPE users have long recognized the variable vaporization rate of solid TMIn. That is, the effective TMIn vapor pressure decreases after about 40% of usage, presumably due to a decreased surface area caused by recrystallization of TMIn inside the bubbler [6, 7]. To alleviate the problems, a special sublimer design is necessary [7]. (2) The methyl radicals produced during TMIn pyrolysis are a likely source for carbon contamination. For example, it has been documented that the methyl radicals from trimethylgallium (TMGa) and trimethylarsine pyrolysis lead to carbon contamination in GaAs as an acceptor impurity [8-10]. For TMIn, the result has been less definitive [11] because of the relatively low carbon concentrations for normal growth conditions [5]. Recently, the question has been clearly resolved for the growth of InAs at low temperatures, where the carbon concentrations are much higher [12, 13]. For InAs epilayers grown using TMIn and $AsH_3$, the carbon concentration detected by secondary ion mass spectroscopy (SIMS) increased as the growth

temperature was reduced [12], with carbon concentrations as high as $10^{19}$ $cm^{-3}$ at 300 °C [12].

In addition to the above problems, TMIn decomposes too slowly for the growth of InAsBi at very low temperatures (<300 °C) [12]. Recently, Bi concentrations as high as 6% have been incorporated into InAs to reduce the energy bandgap of InAs into the 12 μm range [12]. Thus, InAsBi and InAsSbBi become attractive alternative materials for far infrared device applications. However, it is found that growth temperatures as low as 275 °C are necessary in order to incorporate 6% Bi into InAs. At this low growth temperature, TMIn decomposition is not complete [14] so the growth rates of InAs and InAsBi are unacceptably low [12].

This discussion indicates that the development of other indium sources would be beneficial. One possible replacement is ethyldimethylindium (EDMIn) [6, 12, 15]. Since it is a liquid at room temperature, it does not have the problems associated with a variable transport rate. However, it is not certain how ligand exchange reactions [16] affect the final molecules transporting to the crystal growth surface. Moreover, EDMIn has problems with carbon contamination at low temperatures [12], due to the presence of methyl groups. It also decomposes at temperatures too high for the low temperature growth of InAsBi and InAsSbBi [12]. Thus, there remains a need for other indium precursors.

In this work, we report the results of the first study of triisopropylindium [$(C_3H_7)_3In$, TIPIn] as a possible TMIn replacement for OMVPE growth of In-containing materials. Both decomposition and OMVPE growth results are presented.

## 2. EXPERIMENTAL

The general procedure for the TIPIn synthesis is as follows. Organic solvents were distilled under Ar from sodium/benzophenone. Synthesis was carried out under purified Ar using inert atmosphere techniques. Reaction flasks were wrapped in aluminum foil to minimize exposure to light. Air- and moisture-sensitive materials were transferred inside a $N_2$-filled Vacuum Atmospheres glove box. $InCl_3$ (99.999% metal basis) was purchased from Alfa and used as received. (i-Pr)MgCl was purchased from Aldrich Chemical Company and used as received. Nuclear Magnetic Resonance (NMR) spectra were recorded on $C_6D_6$ solutions with an IBM NR-80 spectrometer.

TIPIn was synthesized by reaction of $InCl_3$ with 3.5 equivalents of (i-Pr)MgCl in diethyl ether [17]. The diethyl ether was removed under vacuum and the residue was extracted with hexane. After filtration, the solvents were removed by fractional vacuum distillation and the crude product was collected in a liquid $N_2$ trap. The liquid was then heated to 80-85 °C at 10 torr for 2 hours in the absence of light to remove any traces of solvent. The product was then purified by fractional vacuum distillation two more times (60 °C at 2 torr and 53 °C at 1.2 torr) to yield an air-, heat- and light-sensitive light-yellow pyrophoric liquid. The desired compound was confirmed by $^1H$ and $^{13}C$ NMR spectroscopy.

The TIPIn vapor pressure has been reported to be [18]

$$\log P(\mathrm{Torr}) = 8.453 - 2665.8/T(\mathrm{K}) \quad (1)$$

This gives a value of 0.32 torr at 25 °C. Our distillation values for TIPIn are 2.0 torr at 60 °C, 1.2 torr at 54 °C, and 0.9 torr at 48 °C. These values are consistent

with the more accurate values from equation (1). In the following, equation (1) is used to calculate the TIPIn partial pressures and V/III ratios.

The decomposition experiments were conducted in an isothermal, flow-tube, $SiO_2$ ersatz reactor at atmospheric pressure (635 Torr in Salt Lake City). The diameter and the length of the reactor are 0.4 and 41.5 cm, respectively. The TIPIn source was held at 23 °C and the carrier gas was He with a flow rate of 40 sccm. This gives a residence time of about 3.2 seconds at 300 °C in the hot zone. A schematic diagram of the apparatus has been published previously [19]. Unless specified otherwise, the TIPIn source was purged with He for more than 12 hours before each experiment.

For OMVPE growth of InAs, an atmospheric pressure horizontal reactor was used. The arsenic source was 100% arsine. The cross section of the rectangular reactor was 5 cm wide and 2 cm high. The carrier gas for the sources was palladium-diffused $H_2$ with a total flow rate of about 2.5 liter/min. Separate stainless steel tubing was used for the group III and V reactants in order to minimize possible parasitic reactions. The mixing of the group III and V reactants occurred immediately before entering the quartz reactor. The typical TIPIn flow rate was 300 cc/min with the bubbler being held at 22 °C. The $AsH_3$ flow rate was on the order of 20 cc/min.

Undoped (100) InAs substrates were used. Before growth, the substrates were degreased using trichloroethylene, acetone, and methanol. The substrates were then etched using HF : $H_2O$ = 1 : 1 for 2 minutes and 0.5 % Bromine in methanol for 3 minutes. The surface morphologies of the epilayers were observed using a differential interference contrast microscope. Layer thicknesses, on the order of 1 μm, were determined by observing the

heteroepitaxial interface between the epilayer and the substrate on a cleaved cross-section. When the interface was not readily observable, a diluted A-etch was used to reveal the interface. The crystallinity of the epilayers was verified using x-ray diffraction.

The layers for van der Pauw measurements were grown on semi-insulating InP substrates. The In contacts on the four corners of the rectangular samples were annealed at 300 °C for 1-2 minutes under $N_2$. The magnetic field was 5 kG and the sample current was about 10 µA. For low temperature photoluminescence (PL) measurements, the excitation source was an Argon ion laser operating at 488 nm. The beam was focused to a spot size of approximately 0.5 $mm^2$. The excitation intensity was on the order of 20 $W/cm^2$. The samples were bonded to the cold finger of a closed cycle He cryostat with an IR transmitting $BaF_2$ window. A pair of off-axis paraboloidal reflectors focused the PL onto the entrance slit of a half-meter Spex M500 spectrometer. A GaAs filter was used to block the scattered laser light and to pass the desired radiation. The filter was carefully checked by FT-IR transmittance and was found to be transparent at wavelengths as long as 16 µm. Lock-in techniques were used to detect the PL using an InSb detector cooled to liquid $N_2$ temperature.

## 3. RESULTS AND DISCUSSION

### 3.1 Decomposition

As mentioned in the experimental section, the TIPIn decomposition study was carried out in a flow tube reactor. The temperature was varied from 50 to 200 °C in 25 °C increments. Fig. 1 shows the results at 50 and 200 °C. The signal intensity is weak as compared to, for example, the decomposition results

for TMGa [20]. This is partly due to the low TIPIn vapor pressure at room temperature, giving a low TIPIn partial pressure in the ambient. This is exacerbated by the fact that In sources tend to generally give low signal intensities [21]. The m/e values between 100 and 300 are not shown in Fig.1 because no peaks were observed, including the TIPIn parent peak. Comparing the results in Fig.1 (b) & (c), it is seen that extra peaks are observed at m/e values of 39, 42, 43, 71, and 86 at 200 °C. The peaks at 42 and 43 can also be resolved for spectra obtained at 125, 150, and 175 °C. So, they are not spurious.

The dependence of peak intensity on temperature is plotted in Fig.2 for m/e values of 39, 42, 43, and 71. The intensities increase rapidly from 100 to 125 °C and saturate above 125 °C. The results show that the TIPIn decomposes easily, with a value of $T_{50}$ (temperature for 50% decomposition) of about 110 °C. For comparison, the value of $T_{50}$ obtained for TMIn using identical conditions is about 310 °C [14]. The ease of decomposition is most likely due to the weak In-$C_3H_7$ bond. It is known that the H-alkyl bond strength decreases in the order [22]:

$$CH_3\text{-}H > C_2H_5\text{-}H > i\text{-}C_3H_7 \;.$$

It is expected that the alkyl-In bond strengths follows the same order. In other words, the $C_3H_7$-In bond in TIPIn should be significantly weaker than the $CH_3$-In bond in TMIn. Thus, TIPIn is expected to decompose at lower temperatures than TMIn.

The intensity at m/e=43 is weak at 50 °C. If the undecomposed TIPIn makes its way into the mass spectrometer, the principle peak is expected to be due to $C_3H_7$ at m/e=43. This is, indeed, the case for triisopropylantimony [23].

Thus, the principle peak for TIPIn is not positively observed at 50 °C. As a result, the intensities at m/e=39, 42, 43 come mainly from the decomposition products.

It is difficult to identify the products from Figs.1 and 2 because only a few peaks are well-resolved. Thus, it is not possible to positively determine the TIPIn decomposition mechanism. One possible reaction pathway is β-hydrogen elimination:

$$(C_3H_7)_3In = C_3H_6 + (C_3H_7)_2InH \qquad (2)$$

as has been observed to occur for the decomposition of triethylgallium (TEGa) [24], triethylaluminum (TEAl) [25], and triisobutylaluminum (TIBAl) [26]. Another possibility is homolytic fission:

$$(C_3H_7)_3In = C_3H_7 + (C_3H_7)_2In \qquad (3)$$

The resulting isopropyl radicals may subsequently participate in disproportionation and recombination reactions:

$$C_3H_7 + C_3H_7 = C_3H_6 + C_3H_8 \qquad (4)$$

$$C_3H_7 + C_3H_7 = C_6H_{14} \qquad (5)$$

yielding $C_3H_6$, $C_3H_8$ and $C_6H_{14}$. The fragmentation patterns for these three species [27] are listed in Table 1 for the m/e values of 39, 42, 43, 71, and 86, the well resolved peak positions in this study. From the presence of peaks at m/e=71 and 86, it is clear that $C_6H_{14}$ is produced during TIPIn decomposition. Since the intensities at other peak positions have contributions from $C_3H_6$, $C_3H_8$ and $C_6H_{14}$, it is not possible to definitively identify the presence of $C_3H_6$ and $C_3H_8$. The fragmentation distribution for $C_6H_{16}$ is plotted in Fig.3 for

comparison with the experimental results at 200 °C. The intensity from $C_6H_{14}$ at m/e=71 is made to be equal to the experimental result at m/e=71. It is seen that the $C_6H_{14}$ fragmentation pattern explains the general features of the experimental result. However, it is possible that some of the intensity at m/e=39 is not accounted for by $C_6H_{14}$ alone. Thus, it is possible that small concentration of $C_3H_6$ and/or $C_3H_8$ may be produced from TIPIn decomposition. In terms of the reaction mechanism, the results suggest that the reactions (3) and (5) dominate. It is not certain to what degree reactions (2) and (4) contribute to the TIPIn decomposition.

### 3.2 OMVPE Growth

The OMVPE growth experiments were carried out in a typical OMVPE reactor, as described in the Experimental section. InAs was grown to test the utility of the TIPIn.

Fig.4 shows the surface morphologies of InAs layers grown at 500, 400, and 300 °C, with V/III ratios of about 150. The surface morphology degrades as the growth temperature is lowered. This is not related to the use of TIPIn, but to the incomplete decomposition of $AsH_3$. Since $AsH_3$ decomposes slowly at low growth temperatures [28], the real V/III ratio at the interface may be much smaller than the input V/III ratio. For the sample grown at $T_g$=300 °C and an input V/III ratio of 144, the V/III ratio at the interface is probably less than unity. Thus, the surface appears to be black to the naked eye, due to well-known whisker growth [29, 30]. The surface morphologies for the samples grown at 400 and 300 °C can be improved with an increase in V/III ratio. The results for higher input V/III ratios of 461 are shown in Fig.5 for samples grown at temperatures of 400, 300, and 260 °C. Comparing the results in Figs. 4 and 5, it

is clear that increasing the V/III ratio leads to an improvement of the InAs surface morphology at both 400 and 300 °C. For the growth at 260 °C, even less $AsH_3$ is decomposed. Thus, the input V/III ratio of 461 is not high enough to obtain a good surface morphology. A similar trend of surface morphology dependence upon growth temperature and input V/III ratio has been reported for OMVPE growth of GaInP using $PH_3$ [31] and InP using tertiarybutylphosphine [32].

In order to evaluate the electrical properties using the van der Pauw technique, InAs epilayers were grown on semi-insulating InP substrates. The as-grown epilayers are n-type. Fig.6 shows the room temperature electron concentrations plotted versus growth temperature. The results for InAs grown using TMIn and $AsH_3$ [13] are included for comparison. The electron concentration is about $1\times10^{17}$ $cm^{-3}$ for samples grown at both 500 and 400 °C. This level of impurity concentration is probably caused by background impurities present in the TIPIn source. This is not surprising since the TIPIn is the first bottle ever used for OMVPE growth and is not of electronic grade. It is expected that this background impurity level can be reduced by further purification of the TIPIn. More significant is the increase in electron concentration when the growth temperature falls below 400 °C.

One possible cause for the increase in electron concentration at low growth temperatures is the increased incorporation of a volatile group VI impurity, as has been discussed in Ref. [33]. Another possibility for the increased electron concentration is carbon contamination. Recently, InAs has been grown using TMIn and $AsH_3$ at temperatures as low as 275 °C [12]. It was found that the electron concentration increased as the growth temperature was reduced [12, 13], as shown in Fig.6. The donor impurity has been positively identified as carbon from using SIMS measurements [12, 13]. The

incorporation of carbon as a donor rather than an acceptor (as for GaAs and AlGaAs) has been explained in terms of the relative bond strengths between carbon and the host group III and V atoms [12]. The trend observed for TIPIn is similar to that for InAs grown using TMIn. The major difference is that the electron concentrations for low growth temperatures are much smaller than those for InAs grown using TMIn. This suggest that the donor may be carbon.

As discussed in Section 3.1, TIPIn decomposes mostly by homolysis, that is, by reactions (3) and (5). Thus, free isopropyl radicals are present on the surface. The less reactive isopropyl radicals are expected to result in less carbon incorporation than for $CH_3$. On the other hand, if reaction (2) is the dominant pathway, little carbon contamination would be expected because the reaction product is propene which is unlikely to lead to carbon contamination. For example, methane has been demonstrated to be an ineffective dopant for GaAs [34-35]. In addition, TEGa, which decomposes via the β-hydrogen elimination reaction, has been used to grow GaAs and AlGaAs with very low level of carbon contamination [36].

Fig. 7 shows the growth efficiency as a function of growth temperature. The growth efficiency is defined as the growth rate divided by the group III molar flow rate [37]. The epilayer thickness was measured for InAs grown on InP substrates. The results for InAs and InAsBi grown using TMIn in a similar reactor are also shown for comparison [12]. For the growth of InAs using TIPIn at 300 °C, the growth rate is a nearly linear function of the $H_2$ flow rate (between 0-300 cc/min) through the TIPIn bubbler. It is seen in Fig.7 that the growth efficiency for InAs using TIPIn is only about 700 μm/mole at 500 °C and increases to about 1300 μm/mole at 300 °C. For InAs grown using TMIn and $AsH_3$, the growth efficiency is on the order of $1\times10^4$ μm/mole at high

temperatures where TMIn is completely decomposed [14]. The low growth efficiency for InAs grown using TIPIn may be due to parasitic reactions between TIPIn and $AsH_3$. This has been reported to be the case in the growth of InP and GaInAs using TEIn [38]. Because TIPIn has a low value of $T_{50}$, the low growth efficiency could also be the result of upstream decomposition of TIPIn, resulting in In deposit on the walls. The temperature dependence of the growth efficiency shown in Fig.7 is consistent with either parasitic reactions between TIPIn and $AsH_3$ or premature decomposition of TIPIn upstream of the substrate. In either case, lower growth temperatures would lead to higher growth efficiencies, as observed.

The problem with low growth efficiencies demonstrates the basic difficulty in developing an In precursor for low temperature growth: If the source decomposes at too high a temperature, it is useless for low temperature growth, since it leads to low growth efficiencies. If the value of $T_{50}$ is too low, decomposition occurs inside the bubbler, on the stainless steel tubing, and on the reactor walls upstream of the substrate. This also leads to low growth efficiencies. The low growth efficiency for TIPIn is expected to be alleviated in a low pressure system. It is even less likely to be a problem in chemical beam epitaxy (CBE). In fact, the stability of TIPIn and the absence of $CH_3$ radicals would both seem to be favorable for an In precursor for CBE.

Fig.8 shows the low temperature PL results for samples grown at several temperatures. The PL from an InAs substrate is also shown for comparison. For the InAs substrate, the two low energy peaks at about 3.08 and 3.25 μm have been assigned to emission processes involving either impurity or defect states [39]. The two high energy peaks located near 3 μm are due to band-to-band and exciton recombination [40, 41]. For samples grown using TIPIn and $AsH_3$,

the PL consists mainly of two peaks. The higher energy peak at about 3 μm is apparently due to a combination of peaks from band-to-band and exciton recombination. The lower energy peak at about 3.08 μm is apparently the same impurity/defect peak as for the substrate. The PL intensity is comparable for samples grown at 500 and 400 °C. The PL intensity is much weaker for the sample grown at 300 °C with a V/III ratio of 150. Of course, a V/III of 150 is too low for growth at 300 °C, so a rough surface was obtained, as seen in Fig.4. This may partially explain the low PL intensity. However, even with a V/III of 460, the PL intensity for samples grown at 300 °C is still roughly 60 times weaker than for samples grown at higher temperatures. The observed temperature dependence of PL intensity is similar to that observed for InAs grown using TMIn and $AsH_3$ [13].

## 4. Conclusions

In summary, TIPIn has been investigated as a possible replacement for TMIn in OMVPE growth. From the decomposition study, it is found that TIPIn decomposes with a value of $T_{50}$ of about 110 °C, approximately 200 °C lower than the value for TMIn under similar conditions. The major product is identified as $C_6H_{14}$. The decomposition results suggest that the TIPIn decomposes mainly by homolysis, followed by recombination of the $C_3H_7$ radicals. The growth results show that good surface morphology InAs can be obtained provided that the V/III ratio is sufficiently high. The required V/III ratio has to be increased as the growth temperature is lowered because less $AsH_3$ is decomposed at lower temperatures. The background electron concentration increases as the growth temperature is reduced below 400 °C. The electron concentration is about one order of magnitude smaller using TIPIn than using

TMIn, probably indicating less carbon corporation. The InAs growth efficiency is low. It appears that TIPIn is most useful for low pressure OMVPE or CBE.

## 5. Acknowledgements

The authors would like to thank S.H. Soh and K.T. Huang for assisting with room temperature van der Pauw measurements. Financial support of the this work is provided by the Office of Naval Research, Army Research Office, and Office of Naval Technology.

## 6. References

1. H.M. Manasevit and W.I. Simpson, J. Electrochem. Soc. **120**, 135 (1973).

2. J.P. Duchemin, J.P. Hirtz, M. Razeghi, M. Bonnet, and S.D. Hersee, J. Cryst. Growth 55, 64 (1981).

3. C.P. Kuo, J.S. Yuan, R.M. Cohen, J. Dunn, and G.B. Stringfellow, Appl. Phys. Lett. **44**, 550 (1984).

4. C.C. Hsu, R.M. Cohen, and G.B. Stringfellow, J. Cryst. Growth **63**, 8 (1983).

5. C.H. Chen, M. Kitamura, R.M. Cohen, and G.B. Stringfellow, Appl. Phys. Lett. **49**, 963 (1986).

6. C.P Kuo, R.M. Fletcher, T.D. Osentowski, G.R. Trott, and J.E. Fouquet, paper presented at *The Fourth Biennial Workshop on Organometallic Vapor Phase Epitaxy*, October 8-11, 1989, Monterey, California.

7. AKZO Chemicals Inc., *Newsletter*, October, 1991.

8. T.F. Kuech and E. Veuhoff, J. Cryst. Growth **68**, 148 (1984).

9. J. van de Ven, H.G. Schoot, and L.J. Giling, J. Appl. Phys. **60**, 1648 (1986).

10. R.M. Lum, J.K. Klingert, D.W. Kisker, S.M. Abys, and F.A. Stevie, J. Cryst. Growth **93**, 120 (1988).

11. S. Bose, S. Jackson, A. Curtis, and G. Stillman, paper L2 presented at the 18th International Symposium on GaAs and Related Coumpounds, Sept. 9-12, 1991, held at Seattle, Washington, USA.

12. K.Y. Ma, Z.M. Fang, R.M. Cohen, and G.B. Stringfellow, J. Appl. Phys. **70**, 3940 (1991).

13. Z.M. Fang, K.Y. Ma, R.M. Cohen, and G.B. Stringfellow, Appl. Phys. Lett. **59**, 1446 (1990).

14. N.I. Buchan, C.A. Larsen, and G.B. Stringfellow, J. Cryst. Growth **92**, 591 (1988).

15. K.L. Fry, C.P. Kuo, C.A. Larsen, R.M. Cohen, G.B. Stringfellow, and A. Melas, J. Electon. Mater. **15**, 91 (1986).

16. P.D. Agnello and S.K. Ghanhdi, J. Cryst. Growth **94**, 311 (1989).

17. B.Neumuller, Chem. Ber. **122**, 2283 (1989).

18. V.K. Vanchagova, A.D. Zorin, V.A. Umilin, Zh. Obschei. Khim. **46**, 989 (1976).

19. N.I. Buchan, C.A. Larsen, and G.B. Stringfellow, Appl. Phys. Lett. **51**, 1024 (1987).

20. In this lab, the intensity for TMGa and some other precursors is on the order of $10^{-9}$ amperes, about two orders of magnitude higher than that used in Fig.1.

21. TMIn tends to deposit more on the reactor walls than TMGa. This reduces the amount of TMIn being delivered to the hot zone of the reactor to be pyrolyzed.

22. G.B. Stringfellow, "Organometallic Vapor Phase Epitaxy: Theory and Practice", (Academic Press, New York, 1989), Chapter 2.

23. S.H. Li, C.A. Larsen, G.B. Stringfellow, and R.W. Gedridge, Jr., J. Electron. Mater. **20**, 457 (1991).

24. M. Yoshida, H. Watanabe, and F. Uesugi, J. Electrochem. Soc. **136**, 677 (1985).

25. W.L. Smith and T. Wartik, J. Inorg. Nucl. Chem. **29**, 629 (1967)

26. M.E. Gross, L.H. Dubois, R.G. Nuzzo, and K.P. Cheung, MRS Synposium proceedings, Vol.204, pp383

27. F.W. McLafferty and D.B. Stauffer, The Wiley/NBS Registry of Mass Spectral Data, (Vol.1, John Wiley & Sons, N.Y., 1989)

28. G.B. Stringfellow, "Organometallic Vapor Phase Epitaxy: Theory and Practice", (Academic Press, New York, 1989), Section 4.2.2.1

29. G.B. Stringfellow, "Organometallic Vapor Phase Epitaxy: Theory and Practice", (Academic Press, New York, 1989), pp84-86

30. R.S. Wagner, in "Whiskers Technology", edited by A.P. Levitt (Wiley, New York, 1970)

31. J.S. Yuan, M.T. Tsai, C.H. Chen, R.M. Cohen, and G.B. Stringfellow, J. Appl. Phys. **60**, 1346 (1986)

32. C.H. Chen, D.S. Cao, and G.B. Stringfellow, J. Electron. Mater. **17**, 67 (1988)

33. G.B. Stringfellow, J. Cryst. Growth **75**, 91 (1986)

34. R.M. Lum, J.K. Klingert, D.W. Kisker, D.M. Tennant, M.D. Morris, D.L. Malm, J.Kovalchick, and L.A. Heimbrook, J. Electron. Mater. **17**, 101 (1988)

35. T.F. Kuech, G.J. Scilla, and F. Cardone, J. Cryst. Growth **93**, 550 (1988)

36. T.F. Kuech, Materials Science Reports **2**, 1 (1987)

37. G.B. Stringfellow, "Organometallic Vapor Phase Epitaxy: Theory and Practice", (Academic Press, New York, 1989), Section 1.3

38. C.P. Kuo, Ph.D. Thesis, University of Utah, 1985

39. R.D. Robert, H.D. Drew, J.-I. Chyi, S. Kalem, and H. Morkoc, J. Appl. Phys. **65**, 4079 (1989)

40. A. Mooradian and H.Y. Fan, in "Proceedings of Seventh International Conference on Physics of Semiconductors", Paris, 1964 (Academic, New York, 1965), Vol.4, p.39

41. Z.M. Fang, K.Y. Ma, D.H. Jaw, R.M. Cohen, and G.B. Stringfellow, J. Appl. Phys. **67**, 7034 (1990)

Table 1 Fragmentation Patterns for $C_3H_6$, $C_3H_8$ and $C_6H_{14}$ at several selected m/e values [27]

| m/e | $C_3H_6$ | $C_3H_8$ | $C_6H_{14}$ |
|---|---|---|---|
| | (%) | (%) | (%) |
| 39 | 71.1 | 17.0 | 18.49 |
| 42 | 67.7 | | 84.63 |
| 43 | | 22.8 | 100 |
| 71 | | | 18.94 |
| 86 | | | 4.1 |

Note: The percentage is relative to the principle peak intensity which is taken to be 100 %.

**Figure Captions:**

Fig. 1 Mass spectroscopic results for TIPIn decomposition: (a) background of the mass spectrometer; (b) TIPIn + He at 50 °C; (c) TIPIn + He at 200 °C.

Fig.2 Intensities at several values of m/e versus temperature.

Fig.3 Measured mass spectral intensity distribution at 200 °C compared with that expected for $C_6H_{14}$ [27].

Fig.4 Surface morphology of InAs layers grown on InAs substrates using TIPIn and $AsH_3$ at 500, 400, and 300 °C with V/III ratios of approximately 150.

Fig.5 Surface morphology of InAs layers grown using TIPIn and $AsH_3$ at 400, 300, and 260 °C with V/III ratios of approximately 461.

Fig.6 Room temperature electron concentration for InAs grown using TIPIn and TMIn as a function of growth temperature.

Fig.7 Growth efficiency for InAs grown using TIPIn and $AsH_3$ as a function of growth temperature. The results for InAs and InAsBi grown using TMIn in a similar reactor are also shown for comparison.

Fig.8 Low temperature (10 K) PL spectra for InAs grown using TIPIn and $AsH_3$ at several temperatures. The V/III ratios for the samples shown are about 150. The PL spectrum of an InAs substrate is also shown for comparison.

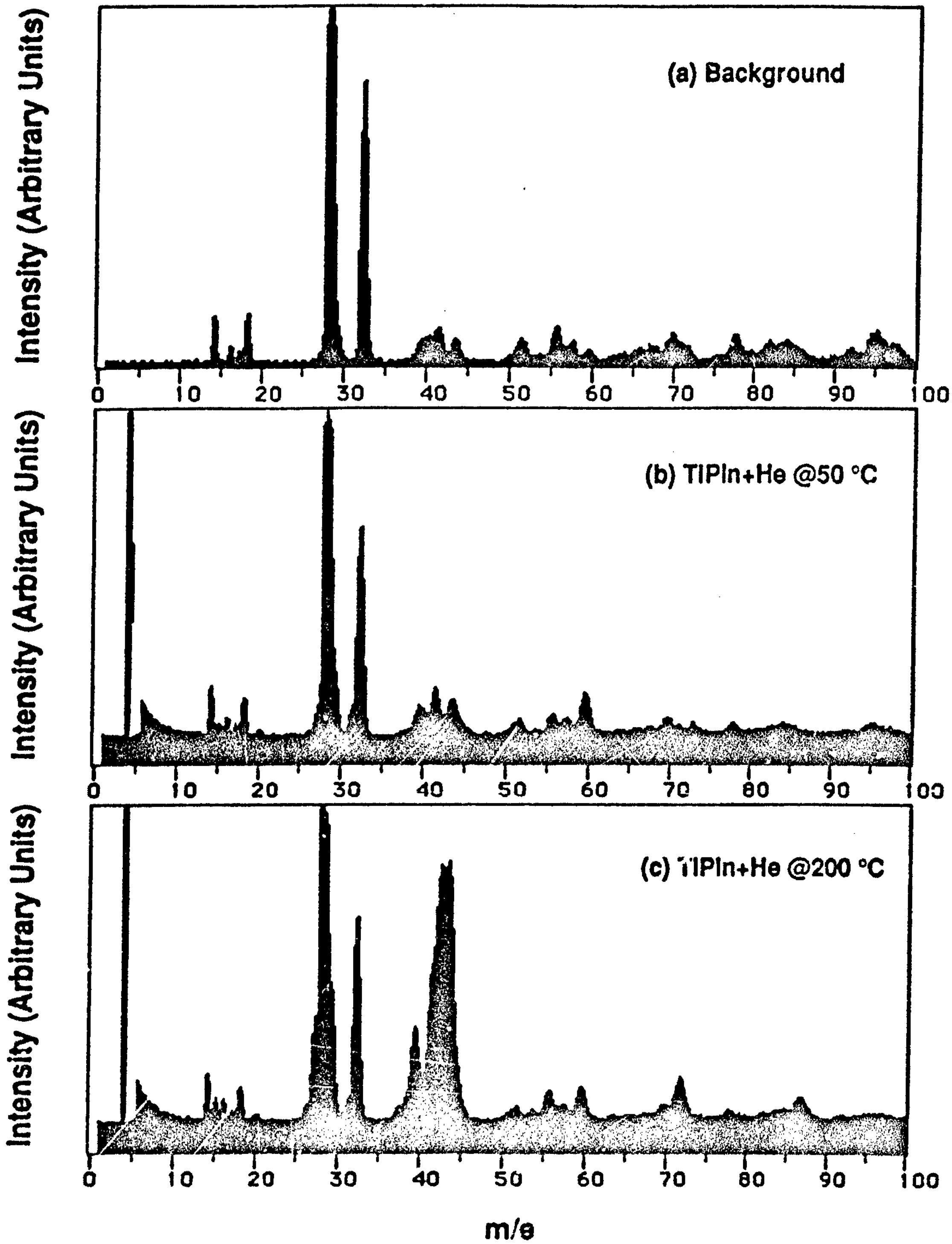

Intensity (Arbitrary Units)
(a) Background
(b) TIPIn+He @50 °C
(c) TIPIn+He @200 °C
0
10
20
30
40
50
60
70
80
90
100
m/e

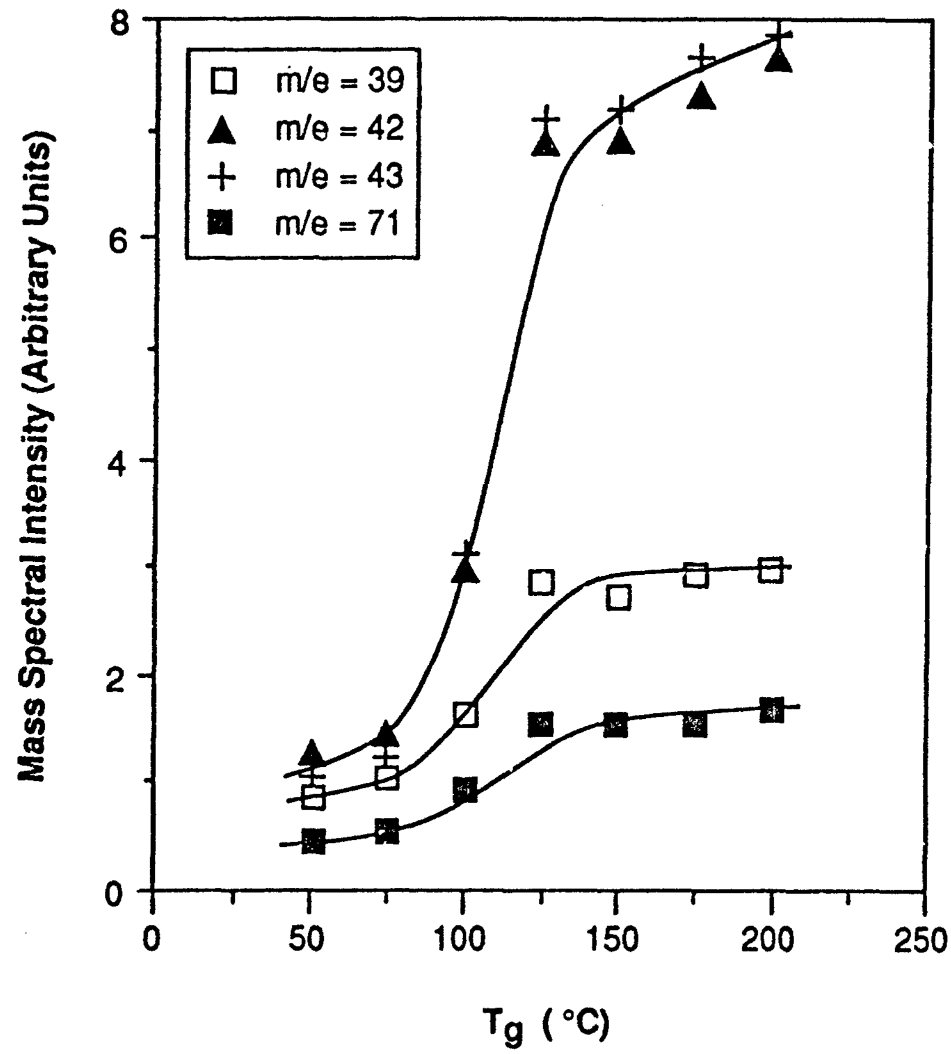

m/e = 39
m/e = 42
m/e = 43
m/e = 71
Mass Spectral Intensity (Arbitrary Units)
0
2
4
6
8
0
50
100
150
200
250
Tg (°C)

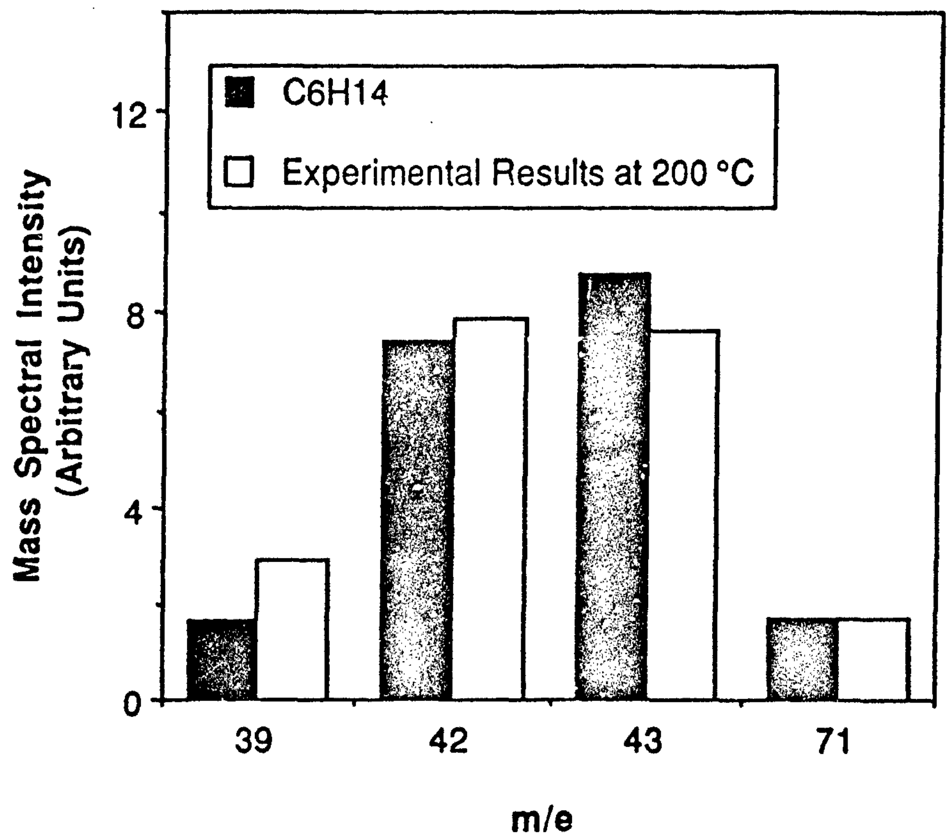
C6H14
Experimental Results at 200 °C
Mass Spectral Intensity (Arbitrary Units)
0
4
8
12
39
42
43
71
m/e

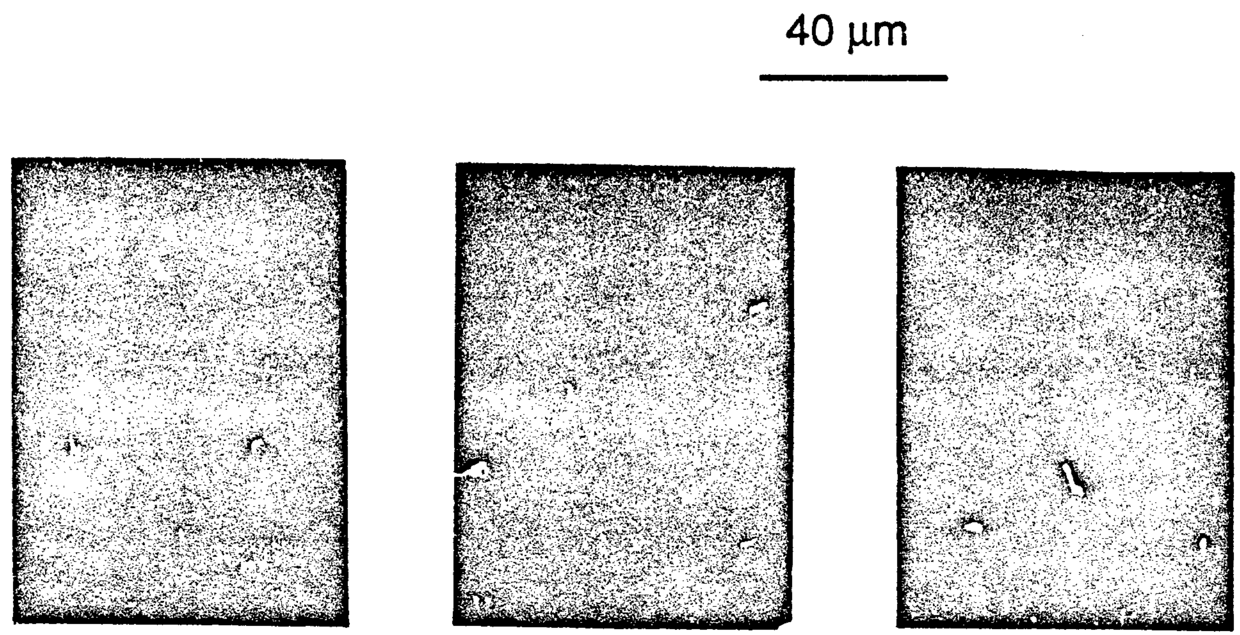


Tg = 500 °C
V/III = 154

Tg = 400 °C
V/III = 165

Tg = 300 °C
V/III = 144

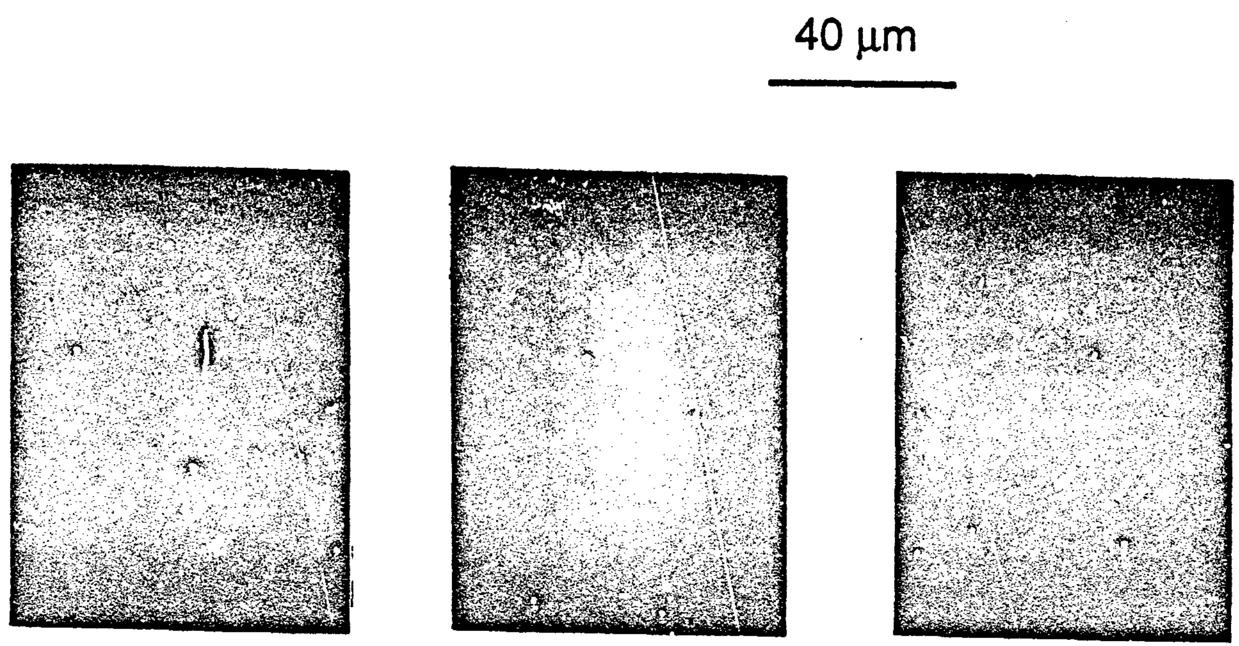


Tg = 400 °C
V/III = 461

Tg = 300 °C
V/III = 461

Tg = 260 °C
V/III = 461

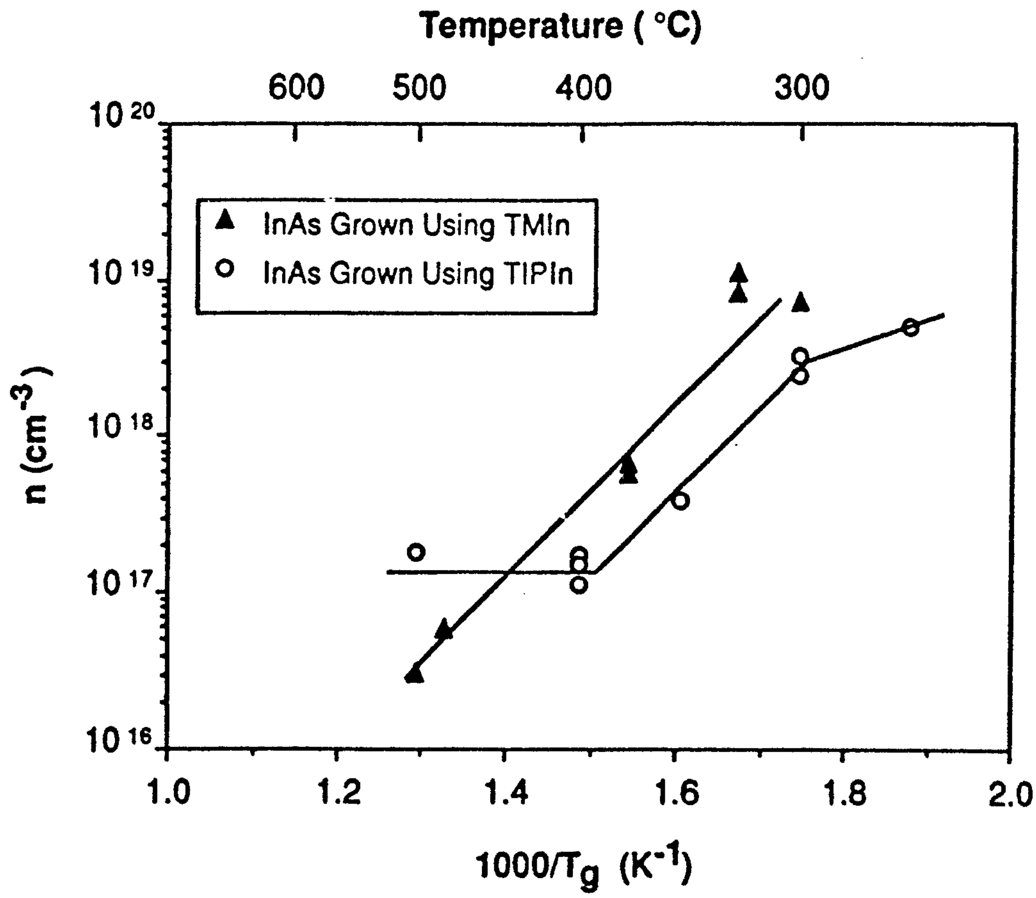

Temperature ( °C)
600
500
400
300
10 20
10 19
10 18
10 17
10 16
n (cm-3)
InAs Grown Using TMIn
InAs Grown Using TIPIn
1.0
1.2
1.4
1.6
1.8
2.0
1000/Tg (K-1)

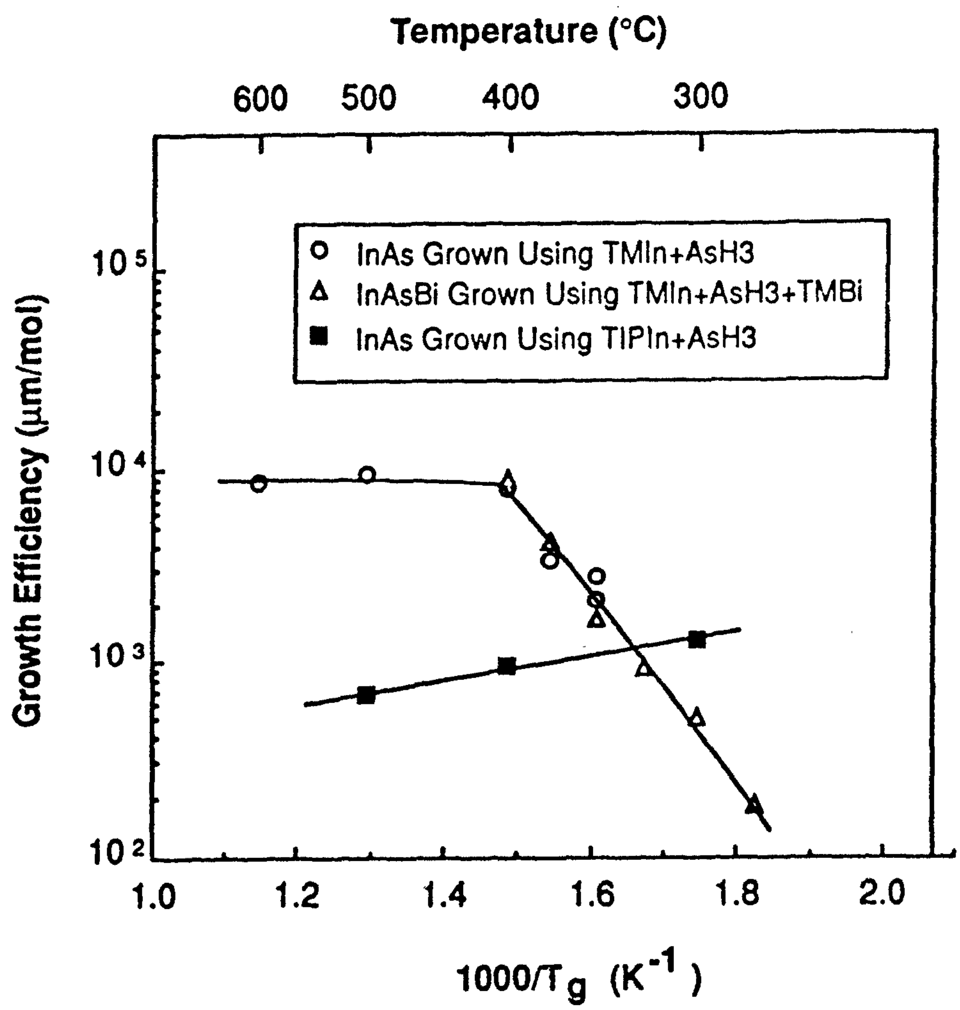

Temperature (°C)
600
500
400
300
InAs Grown Using TMIn+AsH3
InAsBi Grown Using TMIn+AsH3+TMBi
InAs Grown Using TIPIn+AsH3
10 5
10 4
10 3
10 2
Growth Efficiency (µm/mol)
1.0
1.2
1.4
1.6
1.8
2.0
1000/Tg (K-1)

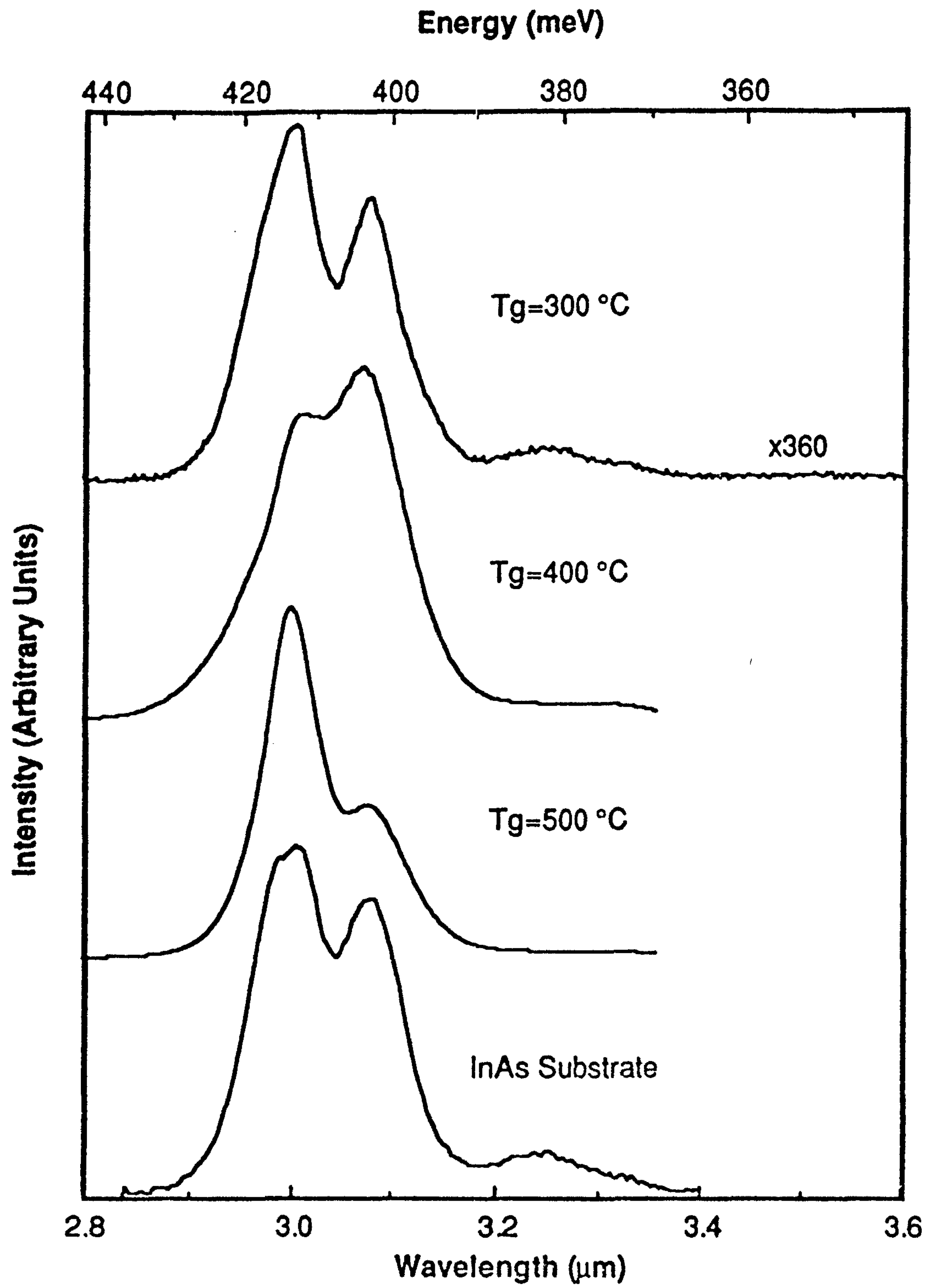
Energy (meV)
440
420
400
380
360
Tg=300 °C
x360
Tg=400 °C
Tg=500 °C
InAs Substrate
Intensity (Arbitrary Units)
2.8
3.0
3.2
3.4
3.6
Wavelength (µm)